MAD preparation of manganites based multilayered structures

Oleg SAPOVAL
Institute of Electronic Engineering and Nanotechnologies, AS RM
shapoval@lises.asm.md

***Abstract* — Metalorganic aerosol deposition is a suitable technique for the synthesis of a wide range of complex oxides thin films. The present paper reports on growth of high quality multilayered structures on the base of functional colossal magnetoresistive manganites layers separated by insulating and metallic oxide spacers. $(La_{0.5}Sr_{0.5}CoO_3\text{-}La_{0.7}Sr_{0.3}MnO_3)_{10}$ and $(SrTiO_3\text{-}LaMnO_3)_{15}$ structures were epitaxially grown on STO(001) and MgO(001) substrates. The evidence for a superlattice formation is confirmed by well-formed satellite peaks in X-ray diffraction and X-ray reflection. The measured periodicities of these superlattices were found to be in good agreement with simulation experiments. The magnetotransport properties of superlattices are presented.**

Index Terms — magnetotransport properties, manganites based superlattices, metalorganic aerosol deposition, XRD and XRR simulations.

I. INTRODUCTION

Manganites still remain during more than ten years one of the most promising classes of functional materials for all-oxide electronics due to wide range of their electrical and magnetic properties [1]. The ideas to build materials with novel or enhanced properties run on engineering of laminate structures which give to developers a large arsenal of tools controlling their properties. Magnetotransport in multilayered structures and superlattices (SL) can be controlled not only by composition of colossal magnetoresistive (CMR) manganites "body" but also by compositional and strain changes on interfaces arisen from substrates [2] and intercalation layers [3]. A combination of CMR manganites with appropriate intercalation layers and substrates allows building spin valve and spinning tunneling devices.

The complex-oxide-based structures are fabricated by the mostly developed thin film growth techniques, like molecular beam epitaxy (MBE) and pulsed laser deposition (PLD). All these techniques possess reasonable stoichiometric and excellent thickness control, when metalorganic chemical vapor deposition (MOCVD) [4] gives an excellent ability governing of complex oxides composition. Developed by our group metalorganic aerosol deposition (MAD) technique [5] adds to conventional MOCVD more flexible work with organic precursors due to transportation of them to the deposition zone at room temperature.

The aim of presented work is demonstration of MAD applicability to deposition of a wide range of composite oxides multilayered structures. Superlattices stacked from CMR $La_{0.67}Sr_{0.33}MnO_3$ (Curie temperature (T_C) 370 K) and metallic $La_{0.5}Sr_{0.5}CoO_3$ (T_C=260K) is a promising candidate to all-oxide spin valve application [1]. Superlattices $SrTiO_3$-$LaMnO_3$ were widely investigetated by numerous researchers [6, 7] and may be important for magnetic tunneling junction applications. The enhancement of functionality in STO-LMO can be achieved by the intentional creation of La- deficiency in LMO individual layers leading to transformation from antiferromagnetic insulator to ferromagnetic metal [8].

The perovskite type STO(001) substrate is attractive as close matched to manganites structure, for LMO the lattice parameter mismatch is about 0.38%. The strain generated by substrate should play the important role in evolution of magnetotransport in epitaxial structures. Whereas it should expect that structures deposited on heavy mismatched MgO substrate will form self-dependent strained structure decoupled from the substrate influence.

II. EXPERIMENTS

Sample preparation: ***Metalorganic Aerosol Deposition*** is a chemical vacuum-free technique, previously engineered for the preparation of high quality oxide thin films and further developed for the deposition of ultrathin films and superlattices [9]. Aerosols of organic solutions, containing metal β- diketonates (e.g. La-, Sr-, Mn-acetylacetonates), are sprayed onto a heated substrate. A film grows on the substrate in a result of a heterogeneous pyrolysis reaction of the metalorganic component. The growth conditions (content of component in solution, molarity, and substrate temperature) for individual layers were defined before SL deposition. The multilayered structures were produced as result of spraying alternating individual portion of solution of respective compounds inputted in spray system. Individual portion were measured out by adjustable micropipette 2-20 µl and 20-200 µl with precision <1%. Such pipette mode has provided a good accurasy in case of used volumes about 200-400 µl corresponding to large period SLs (T≥10 nm). The uniformity of individual impulses of aerosol for short period SLs was founded unsatisfied. The time diagram of aerosol impulses for different modes of deposition is shown in Fig.1. The pipette method gives standard deviation about

This work was supported by DFG (SFB 602) and STCU grant 5390.

5.8%. The dosing unite based on peristaltic pump was proposed to overcome this obstacle. The standard deviation for aerosol impulses with volumes 10-50 µl measured out by peristaltic pump was reduced about an order and was equal to 0.6%.

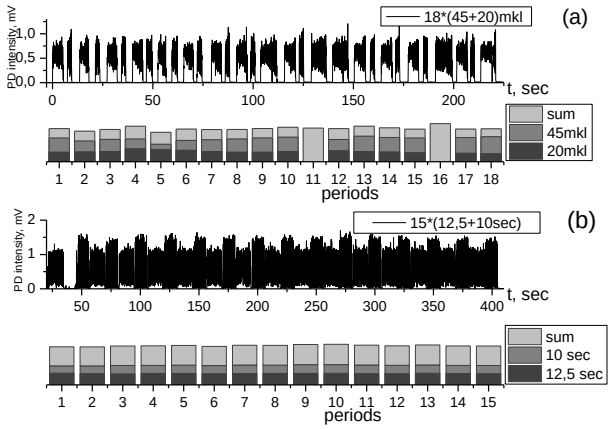

Fig. 1 Diagram of the process of multilayer structures deposition: (a) pipette deposition, (b) peristaltic pump deposition. Registered by PD aerosol impulses and calculated volumes of impulses.

Substrate preparation: The atomically smooth TiO_2-terminated STO(100) substrates with terrace steps of one unit cell in height were obtained by treating the crystal surface with a pH-controlled NH_4F-HF solution [10] followed by annealing at 950ºC before deposition process. The atomically smooth MgO(100) substrates with terrace steps of a half unit cell in height were obtained by annealing directly before deposition at 1050 ºC.

Structures: Single epitaxial LSMO layers exhibit close to bulk material T_C and low resistance at low temperatures. LSCO films demonstrate metallic behavior in temperature range 10-400 K. Multilayered structures $(LSCO\text{-}LSMO)_{10}$ were deposited on STO(001) and MgO(001) substrates by pipette technique from individual portion of 0.01M solution ranged between 90 and 200 µl. Subscript index after brackets denotes the number of periods which were ranged from 4 to 11.5 nm. The substrate temperatures were kept around 980 ºC for MgO and 960 ºC for STO substrates.

Single La-deficient LMO layer deposited on STO substrate shows metal-insulator transition at 330 K and ferromagnetic metallic behavior below this temperature. Multilayered structures $(STO\text{-}LMO)_{15}$ with period 5,6 nm were prepared by peristaltic pump technique. Enhanced accuracy allowed increasing the solution concentration to more preferable 0.02M

*Measurements***:** The film surface morphology was examined by a scanning tunneling microscope (STM) in a Veeco Multimode V Scanning Probe Microscope. The SL structures were determined by a small-angle X-ray reflectivity (XRD) and X-ray diffraction (XRD) in a Siemens D5000 diffractometer. Electron transport measurements were performed by standard 4-probe technique using commercial PPMS from "Quantum Design". Magnetization was measured by means of commercial SQUID (MPMS, "Quantum Design").

III. RESULTS AND DISCUSSION

Structure and morphology. The surfaces of LSCO-LSMO structures deposited on MgO and STO substrates are presented in Fig.2. Scan along indicated direction shows steps equal to perovskite unit cell parameter. The surface of structure grown on MgO substrate reveals leaf-type pattern with terraces ranged from 20 to50 nm and roughness 0.38 nm. The surface of structure deposited on STO demonstrates wide (up to 200 nm) meandered terraces.

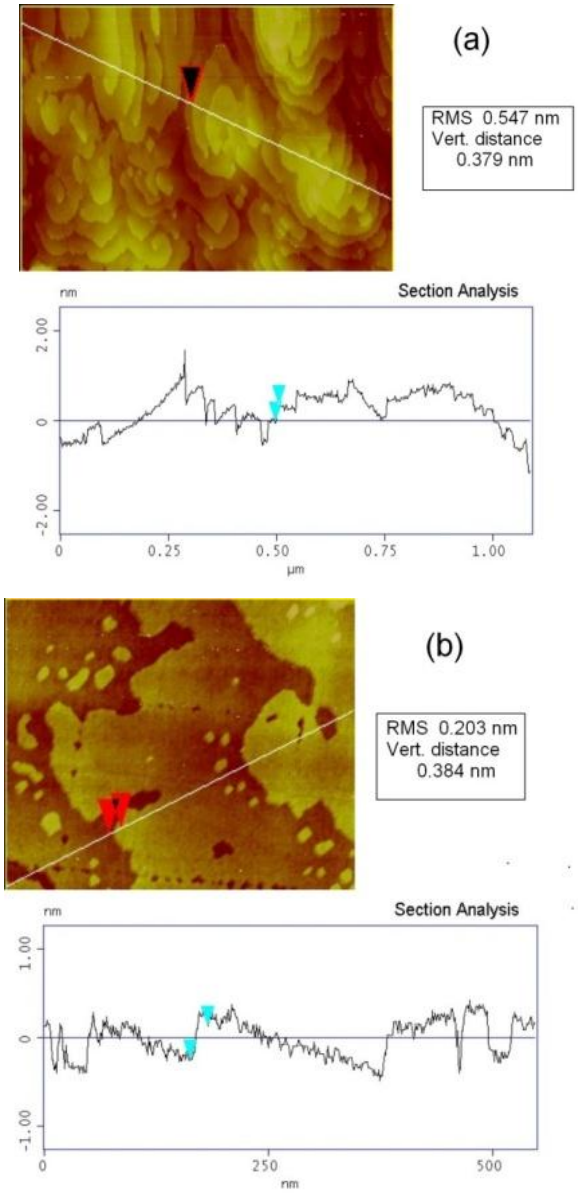

Fig. 2 STM images and analysis of the (LSCO-LSMO)10 superlattices surface deposited on: (a) MgO(001) and (b) STO(001) substrates.

The STM investigation of STO-LMO SL shows more developed than for LSCO-LSMO surface with RMS >1 nm (image isn't presented here). A progressive increase in interface roughness at growth is specified for stacked two perovskites with different cation valence and is a sequence of polarity interfaces [11].

The evidence for a SL formation is confirmed by well-formed satellite peaks for all prepared structures. The SL periods were calculated from satellite peak positions [12]

as well as from XRR peak positions [13]. Fig.3 shows θ-2θ X-ray diffraction spectra measured around the (001) Bragg peak for the STO-LMO SLs. The simulations of XRD and XRR curves were performed using on-line calculation provided by X-Ray Server (S.Stepanov: http://sergey.gmca.aps.anl.gov). In simulation routine we used the value of period calculated from experimental curve. The individual thicknesses of component were taken into account around mean value of period in accordance of deviation registered during deposition process (Fig.1). Adjusting curve were performed by variation individual thicknesses, strain parameter (da/a) and roughness. Due to small number of repetition (15 periods) the structure were presented as 30 individual layers with their own parameter. The roughness was gradually increased from 0.1 nm for bottom layer to 1.0 nm for top layer as specified for substrate and whole structure from STM measurement. The calculated SL0 peak position (hidden on experimental curve by STO(001) diffraction peak) is moved to bigger angle indicating reduction of average SL parameter relative to STO. Strain da/a=-0.004 in LMO was generated by STO substrate and maintained by intercalation STO layers. Besides strain in LMO layers the thicknesses of LMO layers (mean value 4.2 nm) and STO layers (mean value 1.6 nm) components were defined.

Peak SL0 from SL grown on MgO substrate demonstrates shift to smaller angle relative STO(001) position.

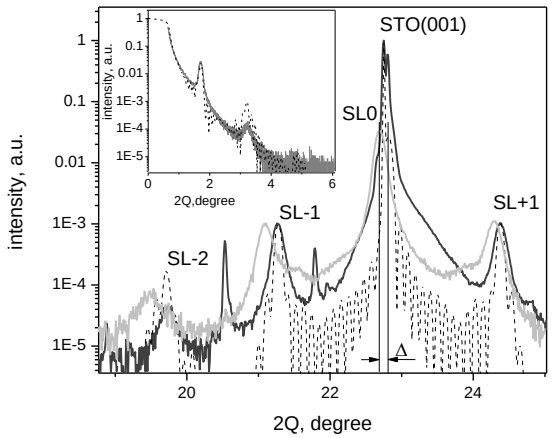

Fig. 3 X-ray diffraction curve (dark grey) and simulation (dotted) around (001) reflex of $(STO\text{-}LMO)_{15}$ SL grown on STO(001) substrate. Δ denotes shift between SL0 peak positions of SLs grown on STO and MgO (light grey). The insert shows experimental (grey) and simulated (dotted) X-ray small angle reflection.

This result suggests that the STO layers in the STO-LMO SL grown on MgO substrate were compressively strained (da/a=0.001), leading to a slight elongation of the out-of-plane lattice constant.

Magnetotransport properties. Fig.4 presents magnetotransport properties of $(LSCO\text{-}LSMO)_{10}$ SLs grown on STO and MgO substrates. The M vs T curve clearly indicates two transitions. The T_C of LSMO is around 335 K, lower than the bulk value. The T_C of LSCO is near 260 K corresponds to the bulk value. The ferromagnetic hysteresis loop at 10 K shows only one transition corresponding to simultaneous switching of the whole structure, although, at list two magnetic phases are observed. The ferromagnetism at room temperature and the difference in the Curie temperatures is an important prerequisite to the fabrication of an all-oxide GMR structure. The R vs H dependence reflects the domination of CMR effect. The further individual component thickness optimization is required to enhance the low field magnetoresistance.

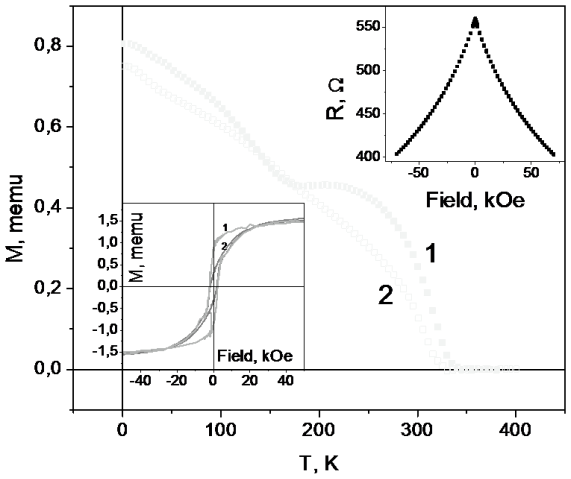

Fig. 4 Magnetization as a function of temperature with an applied magnetic field of 1000 Oe for the $(LSCO\text{-}LSMO)_{10}$ SL grown on STO (1) and MgO (2) substrates. Top insert: resistance as function of applied field measured at 300 K. Bottom insert: magnetic hysteresis measured at 10 K.

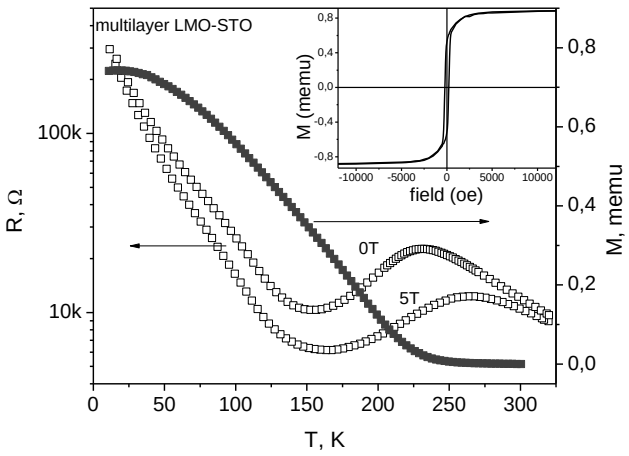

Fig. 5 Dependence of transport properties and magnetization on temperature for $(STO\text{-}LMO)_{15}$ SL grown on STO subsrate. Insert shows magnetic hysteresis loop measured at 10 K.

Magnetotransport properties of $(STO\text{-}LMO)_{15}$ grown on STO substrate is summarized in Fig. 5 for SL with period 5.8 nm and relation of individual component 4 ML STO and 11 ML LMO. Hysteresis loops measured at 10 K and resistivity curves evidence ferromagnetism in the sample. The ferromagnetism and transition to metallic state is most

probably due to La deficiency [8] intentionally generated in LMO layers. Relatively low transition and Curie temperature around 230 K can be explained by lowering concentration of Mn^{4+} ions and/or strain in LMO layers [6] evident from XRD analysis. Very low value of a saturation magnetic moment 1.8 μ_B/Mn at 10 K argues in favor of insufficient doping level of manganite [14]. Contrary to SL grown on STO structure the structure deposited on MgO substrate demonstrates an insulating behavior in whole temperature range. The forming of La-deficient LMO is possible due to epitaxial stabilization of a nonstoichiometric state in the strained layers grown on $SrTiO_3$ (STO) (100) substrates [8]. Fully relaxed LMO layers grows stoichiometric respect to ratio La/Mn and therefore is antiferromagnetic and insulating [15].

IV. CONCLUSION

Metalorganic aerosol deposition allows the synthesis of a wide range of complex oxides thin films with various functionalities. Above all it offers a flexible tool for engineering of stacked structures due to manipulations with solution composition. SLs prepared by MAD demonstrate the structural quality consistent with PLD grown structures. The epitaxial growth of manganites based superlattices is possible on matched STO as well as on heavy mismatched MgO substrates. It worth mentioning that great work on optimization functional properties of proposed structures is required.

ACKNOWLEDGMENTS

The author acknowledges the S.Stepanov's project X-Ray Server provided free online access to X-ray data analysis programs.

REFERENCES

[1] T. Venkatesan, *et al.*, "Manganite-based devices: opportunities, bottlenecks and challenges," *Philosophical Transactions of the Royal Society of London. Series A: Mathematical, Physical and Engineering Sciences*, vol. 356, pp. 1661-1680, July 15, 1998 1998.

[2] Y. M. Xiong, *et al.*, "Magnetotransport properties in $La_{1-x}Ca_xMnO_3$ (x = 0.33, 0.5) thin films deposited on different substrates," *Journal of Applied Physics*, vol. 97, pp. 083909-11, 2005.

[3] G. Rijnders and D. H. A. Blank, "Materials science: Build your own superlattice," *Nature*, vol. 433, pp. 369-370, 2005.

[4] P. J. Wright, *et al.*, "Metal organic chemical vapor deposition (MOCVD) of oxides and ferroelectric materials," *Journal of Materials Science: Materials in Electronics*, vol. 13, pp. 671-678, 2002.

[5] V. Moshnyaga, *et al.*, "Preparation of rare-earth manganite-oxide thin films by metalorganic aerosol deposition technique," *Applied Phsysics Letters*, vol. 74, pp. 2842-2844, 1999.

[6] J. Garcia-Barriocanal, *et al.*, "'"Charge Leakage" at $LaMnO_3/SrTiO_3$ Interfaces," *Advanced Materials*, vol. 22, pp. 627-632, 2010.

[7] W. S. Choi, *et al.*, "Charge states and magnetic ordering in LaMnO3/SrTiO3 superlattices," *Physical Review B*, vol. 83, p. 195113, 2011.

[8] A. Gupta, *et al.*, "Growth and giant magnetoresistance properties of La-deficient $La_xMnO_{3-\delta}$(0.67< x <1) films," *Applied Physics Letters*, vol. 67, pp. 3494-3496, 1995.

[9] K. Gehrke, *et al.*, "Interface controlled electronic variations in correlated heterostructures," *Physical Review B*, vol. 82, p. 113101, 2010.

[10] M. Kawasaki, *et al.*, "Atomic Control of the SrTiO3 Crystal Surface," *Science*, vol. 266, pp. 1540-1542, December 2, 1994 1994.

[11] N. Nakagawa, *et al.*, "Why some interfaces cannot be sharp," *Nat Mater*, vol. 5, pp. 204-209, 2006.

[12] P.F.Fewster, Ed., *X-Ray and Neutron Dynamical Diffraction*. Plenum Press, New York, 1996, p.286.

[13] M. Sugawara, *et al.*, "Exact determination of superlattice structures by small-angle x-ray diffraction method," *Applied Physics Letters*, vol. 52, pp. 742-744, 1988.

[14] C. Adamo, *et al.*, "Electrical and magnetic properties of $(SrMnO_3)_n/(LaMnO_3)_{2n}$ superlattices," *Applied Physics Letters*, vol. 92, pp. 112508-3, 2008.

[15] A. Yamasaki, *et al.*, "Pressure-Induced Metal-Insulator Transition in $LaMnO_3$ Is Not of Mott-Hubbard Type," *Physical Review Letters*, vol. 96, p. 166401, 2006.